Some notes on the "inch-worm model"

J. Bratt, B. van de Sande, and E. M. Watson
Geneva College
3200 College Ave., Beaver Falls, PA 15010

These are our results for the analysis of the "inch-worm model." [1] We wrote down the bound state equation with rotational symmetries included explicitly. We then analyzed the small Bjorken-x behavior of the wavefunctions.

Basis of states

In order to untangle the helicity structure, I introduce fermion spinors

$$u = \begin{pmatrix} u_+ \\ u_- \end{pmatrix} \quad v = \begin{pmatrix} v_+ \\ v_- \end{pmatrix} \tag{1}$$

and Pauli matrices which act on these spinors,

$$\bar{\Psi}\Psi = -\frac{1}{\sqrt{2}}\left(u^\dagger \sigma^1 v + v^\dagger \sigma^1 u\right) \tag{2}$$
$$\bar{\Psi}\gamma^+\Psi = u^\dagger u \tag{3}$$
$$\bar{\Psi}\gamma^-\Psi = v^\dagger v \tag{4}$$
$$\bar{\Psi}\gamma^1\Psi = \frac{1}{\sqrt{2}}\left(u^\dagger \sigma^3 v + v^\dagger \sigma^3 u\right) \tag{5}$$
$$\bar{\Psi}\gamma^2\Psi = \frac{i}{\sqrt{2}}\left(v^\dagger u - u^\dagger v\right) . \tag{6}$$

I introduce the matrices ζ^λ which also act on the spinors:

$$\begin{array}{c|cccc} \lambda & 1 & 2 & -1 & -2 \\ \hline \zeta^\lambda & \sigma^2 & -\sigma^1 & -\sigma^2 & \sigma^1 \; . \end{array} \tag{7}$$

Using this notation, the pion state can be written as

$$\begin{aligned} |\psi, p^+\rangle \;=\; & \sqrt{\frac{p^+}{2N}} \int_0^1 dx\, \psi(x)\, b^\dagger(xp^+)\, \sigma^2 d^\dagger((1-x)p^+)\, |0\rangle \\ & + \frac{p^+}{\sqrt{8}N} \int_0^1 dx \int_0^{1-x} dy \sum_\lambda \Big\{ \psi_S(x,y)\, b^\dagger(xp^+)\, \sigma^2\, a_\lambda^\dagger(yp^+)\, d^\dagger((1-x-y)p^+) \\ & + \psi_A(x,y)\, b^\dagger(xp^+)\, \zeta^\lambda \sigma^2\, a_\lambda^\dagger(yp^+)\, d^\dagger((1-x-y)p^+) \Big\} |0\rangle \end{aligned} \tag{8}$$

To obtain the $J_z = 0$ component of the rho, replace $\sigma^2 \to \sigma^1$ in the above. The wavefunctions of the $J_z = \pm 1$ components of the rho are more complicated:

$$|\psi, p^+\rangle = \sqrt{\frac{p^+}{2N}} \int_0^1 dx\, \psi(x)\, b^\dagger(xp^+)\, \sigma^3 d^\dagger((1-x)p^+)\, |0\rangle$$

[1] S. Dalley, Phys. Rev. **D64** (2001) 036006; `http://arXiv.org/abs/hep-lat/0010082`.

$$+\frac{p^+}{\sqrt{8N}}\int_0^1 dx\int_0^{1-x} dy\,\sum_\lambda\Big\{\psi_S(x,y)\,b^\dagger(xp^+)\,\sigma^3\,a^\dagger_\lambda(yp^+)\,d^\dagger((1-x-y)p^+)$$
$$+\psi_A(x,y)\,b^\dagger(xp^+)\,\zeta^\lambda\sigma^3\,a^\dagger_\lambda(yp^+)\,d^\dagger((1-x-y)p^+)$$
$$+\psi'_A(x,y)\,b^\dagger(xp^+)\,\sigma^1\zeta^\lambda\sigma^1\sigma^3\,a^\dagger_\lambda(yp^+)\,d^\dagger((1-x-y)p^+)\Big\}\,|0\rangle\ . \tag{9}$$

This is the state that is odd under reflections $\mathcal{P}^1:\ x^1\to -x^1$; the even state is obtained by removing the σ^3.

The bound state equations are almost identical for the four states. The two-particle bound state equation is

$$\begin{aligned}\mathcal{M}^2\psi(x) \;=\;& \frac{\mu_F^2}{x(1-x)}\,\psi(x)+\frac{(\kappa_S^2+\kappa_A^2)N}{\pi}\left[\int_0^x\frac{dy}{xy}+\int_0^{1-x}\frac{dy}{(1-x)y}\right]\psi(x)\\
&-\frac{G^2}{2\pi}\int_0^1\frac{dy}{(x-y)^2}\,(\psi(y)-\psi(x))\\
&-\frac{\mu_F\kappa_S\sqrt{N}}{\sqrt{\pi}}\left[\int_0^x dy\,\frac{(2x-y)\,\psi_S(x-y,y)}{\sqrt{y}\,x(x-y)}+\int_0^{1-x}dy\,\frac{(2-2x-y)\,\psi_S(x,y)}{\sqrt{y}(1-x)(1-x-y)}\right]\\
&+\frac{\mu_F\kappa_A\sqrt{N}}{\sqrt{\pi}}\left[\int_0^x dy\,\frac{\sqrt{y}\,\psi_A(x-y,y)}{x(x-y)}\right.\\
&\left.+\int_0^{1-x}dy\,\frac{\sqrt{y}}{(1-x)(1-x-y)}\left\{\begin{array}{ll}\psi_A(x,y) & \text{for pion}\\ -\psi_A(x,y) & \text{for rho, } J_z=0\\ -\psi'_A(x,y) & \text{for rho, } J_z=\pm1\end{array}\right.\right]\ ,\end{aligned} \tag{10}$$

where $G^2\equiv g^2(N^2-1)/N$.

For each of the wavefunctions, ψ_S, ψ_A, ψ'_A, three-particle bound state equation is

$$\begin{aligned}\mathcal{M}^2\psi(x,y) \;=\;& \mu_F^2\left(\frac{1}{x}+\frac{1}{1-x-y}\right)\,\psi(x,y)+\frac{\mu_B^2}{y}\,\psi(x,y)\\
&-\frac{G^2}{4\pi}\left[\int_0^{x+y}dz\,\frac{y+z}{\sqrt{yz}(y-z)^2}\,\psi(x+y-z,z)\right.\\
&+\int_0^{1-x}dz\,\frac{y+z}{\sqrt{yz}(y-z)^2}\,\psi(x,z)\\
&\left.-2\psi(x,y)\left(\frac{2}{y}+\int_0^{x+y}\frac{dz}{(y-z)^2}+\int_0^{1-x}\frac{dz}{(y-z)^2}\right)\right]\ .\end{aligned} \tag{11}$$

For $\psi_S(x,y)$, we include

$$-\frac{\mu_F\kappa_S\sqrt{N}}{\sqrt{\pi y}}\left[\frac{2x+y}{x(x+y)}\,\psi(x+y)+\frac{2-2x-y}{(1-x)(1-x-y)}\,\psi(x)\right]\ . \tag{12}$$

For $\psi_A(x,y)$ in the pion and the rho $J_z=0$ state, we include

$$+\frac{\mu_F\kappa_A\sqrt{Ny}}{\sqrt{\pi}}\left[\frac{\psi(x+y)}{x(x+y)}+\frac{1}{(1-x)(1-x-y)}\left\{\begin{array}{ll}\psi(x) & \text{for pion}\\ -\psi(x) & \text{for rho}\end{array}\right.\right]\ . \tag{13}$$

For $\psi_A(x,y)$ in the rho $J_z = \pm 1$ states, we include

$$+\frac{\mu_F \kappa_A \sqrt{N y}\, \psi(x+y)}{\sqrt{\pi} x (x+y)} \; . \tag{14}$$

For $\psi'_A(x,y)$ in the rho $J_z = \pm 1$ states, we include

$$-\frac{\mu_F \kappa_A \sqrt{N y}\, \psi(x)}{\sqrt{\pi}(1-x)(1-x-y)} \; . \tag{15}$$

Endpoint analysis

Next, we analyze the behavior of the wavefunctions as one or more of the momenta go to zero. We will consider each of the following limits:

$$\begin{aligned}
\lim_{\substack{x\to 0,\\ y\text{ constant}}} \psi(x,y) &= x^a g(y) && (16)\\
\lim_{\substack{y\to 0,\\ x\text{ constant}}} \psi(x,y) &= y^\beta g'(x) && (17)\\
\lim_{\substack{x+y\to 0,\\ x/y\text{ constant}}} \psi(x,y) &= (x+y)^b f\left(\frac{x}{x+y}\right) = p^b f(w) && (18)\\
\lim_{x\to 0} \psi(x) &= C_2\, x^\alpha \; , && (19)
\end{aligned}$$

where $x \equiv wp$, and $y \equiv (1-w)p$.

Three particle equation, limit $x \to 0$:

$\psi_S(x,y)$:

$$\begin{aligned}
0 &= \mu_F^2\; g_S(y)\, x^{a-1} - \frac{\mu_F \kappa_S \sqrt{N}}{\sqrt{\pi y}} \psi(y) x^{-1} \\
&\quad - \frac{G^2}{4\pi} \int_0^{x+y} \frac{\mathrm{d}z}{(y-z)^2} \left[\frac{y+z}{\sqrt{yz}} \psi(x+y-z) - 2\psi(x,y) \right] \\
&\quad + O(x^a).
\end{aligned} \tag{20}$$

$\psi_A(x,y)$:

$$\begin{aligned}
0 &= \mu_F^2\; g_A(y)\, x^{a-1} + \frac{\mu_F \kappa_A \sqrt{N}}{\sqrt{\pi y}} \psi(y) x^{-1} \\
&\quad - \frac{G^2}{4\pi} \int_0^{x+y} \frac{\mathrm{d}z}{(y-z)^2} \left[\frac{y+z}{\sqrt{yz}} \psi(x+y-z) - 2\psi(x,y) \right] \\
&\quad + O(x^a).
\end{aligned} \tag{21}$$

In order to cancel the second term we set $a = 0$. We then find that the integral term, which is also $O(x^{a-1})$, goes to zero. Simplifying, we get:

$$g_S(y) = \frac{\kappa_S \sqrt{N}}{\mu_F \sqrt{\pi y}} \psi(y) \tag{22}$$

$$g_A(y) = -\frac{\kappa_A \sqrt{N}}{\mu_F \sqrt{\pi y}} \psi(y) \, . \tag{23}$$

Three particle equation, limit $y \to 0$:

For this limit, the resulting equation is the same for ψ_S and ψ_A because the differing terms are non-leading.

$$\begin{aligned} 0 = & \left(\mu_B^2 + \frac{G^2}{\pi}\right) g'(x)\, y^{\beta-1} \\ & -\frac{G^2}{4\pi} y^{-1} \left[\int_0^{1/y} \frac{\mathrm{d}q}{(1-q)^2} \left[\frac{1+q}{\sqrt{q}} (qy)^\beta g'(x) - 2y^\beta g'(x) \right] \right. \\ & \left. + \int_0^{1/y} \frac{\mathrm{d}q}{(1-q)^2} \left[\frac{1+q}{\sqrt{q}} (qy)^\beta g'(x) - 2y^\beta g'(x) \right] \right] \\ & + O(y^{-\frac{1}{2}}). \end{aligned} \tag{24}$$

We note the constraint $\beta < \frac{1}{2}$ so that the integrals converge and the $O(y^{-\frac{1}{2}})$ terms are non-leading. We also have the constraint $\beta > 0$ so that the wavefunction is bounded. We obtain:

$$\begin{aligned} 0 = & \left(\mu_B^2 + \frac{G^2}{\pi}\right) g'(x)\, y^{\beta-1} \\ & -\frac{G^2}{4\pi} g'(x)\, y^{\beta-1} \; 2 \left[2\pi\beta \tan(\pi\beta) + 2 \right] \; , \end{aligned} \tag{25}$$

Simplifying we get:

$$0 = \left[\mu_B^2 - G^2 \beta \tan(\pi\beta)\right] g'(x)\, y^{\beta-1}. \tag{26}$$

Note that $g'(x)$ is not fixed by this analysis. The value of β in (26) matches the expression found for the two-gluon bound state equation.

Three particle equation, limit $x + y \to 0$, x/y constant

In this limit, we obtain, for both $f_S(w)$ and $f_A(w)$:

$$\begin{aligned} 0 = & \frac{\mu_F^2 \, f_S(w)}{w} p^{b-1} + \frac{(\mu_B^2 + \frac{G^2}{\pi})\, f_S(w)}{1-w} p^{b-1} \\ & -\frac{G^2}{4\pi} p^{b-1} \int_0^1 \frac{\mathrm{d}q}{(q-w)^2} \left[\frac{(2-w-q)\, f_S(q)}{\sqrt{(1-w)(1-q)}} - 2\, f_S(w) \right] \end{aligned}$$

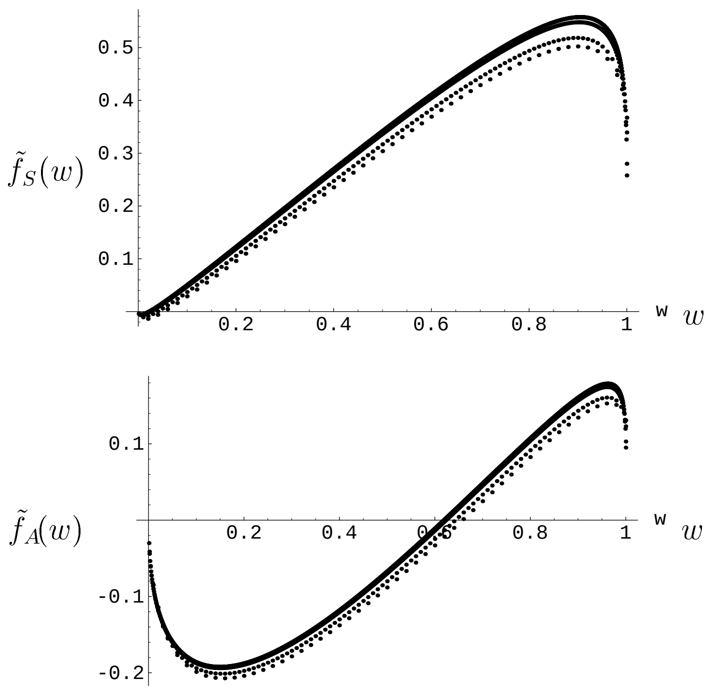

Figure 1: $\tilde{f}_S(w)$ and $\tilde{f}_A(w)$ vs. w for couplings $\mu_F = 0.362G$, $\mu_B = 0.2G$, and $\alpha = 0.4$; results for K= 50, 100, 500, and 1000 are shown.

$$
\begin{aligned}
&-\frac{G^2}{4\pi}\, p^{b-1}\int_0^1 \frac{dq}{(q-w)^2}\left[\frac{(w+q-2qw)\, f_S(q)}{\sqrt{(1-w)(1-q)}}\left(\frac{w}{q}\right)^{\alpha} - 2w\, f_S(w)\right] \\
&\frac{\mu_F C_2\sqrt{N}}{\sqrt{\pi}w}\, p^{\alpha-3/2}\begin{cases} -\kappa_S\frac{(w+1)}{\sqrt{1-w}} & \text{for } f_S(w) \\ \kappa_A\sqrt{1-w} & \text{for } f_A(w)\end{cases} \\
&+O\left(p^{-1/2}\right)\ . \qquad (27)
\end{aligned}
$$

In order for the last term in the equation to be canceled in the limit $p \to 0$, we must set $b = \alpha - \frac{1}{2}$.

These integral equations must be solved numerically. To find the functions $f_S(w)$ and $f_A(w)$ we wrote them as a sum

$$
f_S(w) = \frac{\kappa_S\sqrt{N}C_2}{\mu_F\sqrt{\pi}}(1-w+\tilde{f}_S(w)) \qquad \text{and} \qquad (28)
$$

$$
f_A(w) = -\frac{\kappa_A\sqrt{N}C_2}{\mu_F\sqrt{\pi}}(1-w+\tilde{f}_A(w))\ . \qquad (29)
$$

and computed $\tilde{f}(w)$ numerically. This decomposition was not necessary but the separation will be useful later when substituting the result back into the two particle equation. Equation (27) then has the form:

$$
\frac{\mu_F^2\tilde{f}(w)}{w} + \frac{(\mu_B^2+\frac{G^2}{\pi})\,\tilde{f}(w)}{1-w}
$$

$$
\begin{aligned}
& -\frac{G^2}{4\pi}\int_0^1 \frac{\mathrm{d}q}{(q-w)^2}\left[\frac{\tilde{f}(q)\left(2-w-q+(w+q-2wq)\left(\frac{w}{q}\right)^\alpha\right)}{\sqrt{(1-w)(1-q)}} - 2(1+w)\tilde{f}(w)\right] \\
= & -\frac{\mu_F^2(1-w)}{w} - \mu_B^2 - \frac{G^2}{\pi} + \frac{\mu_F^2}{\sqrt{w}}\begin{cases} \frac{(w+1)}{\sqrt{1-w}} & \text{for } \tilde{f}_S(w) \\ \sqrt{1-w} & \text{for } \tilde{f}_A(w) \end{cases} \\
& +\frac{G^2}{4\pi}\int_0^1 \frac{\mathrm{d}q}{(q-w)^2}\left[\sqrt{\frac{1-q}{1-w}}\left(2-w-q+(w+q-2wq)\left(\frac{w}{q}\right)^\alpha\right) - 2(1-w^2)\right]
\end{aligned} \tag{30}
$$

Both $f_S(w)$ and $f_A(w)$ go to zero in the limits $w \to 0$ and $w \to 1$. For the numerical computation, we discretized w on the interval [0,1], using K points.

Two particle equation, limit $x \to 0$:

$$
\begin{aligned}
0 = & \ \mu_F^2 C_2 x^{\alpha-1} - \frac{G^2 C_2}{2\pi}\left(1-\pi\alpha\cot(\pi\alpha)\right)x^{\alpha-1} \\
& +x^{\alpha-1}\int_0^1 \frac{\mathrm{d}z}{1-z}\left[\frac{\kappa_S^2 N C_2}{\pi} - \frac{\mu_F \kappa_S \sqrt{N}}{\sqrt{\pi}}\left(\frac{(2-z)\, f_S(1-z)}{\sqrt{z}}\right)\right] \\
& +x^{\alpha-1}\int_0^1 \frac{\mathrm{d}z}{1-z}\left[\frac{\kappa_A^2 N C_2}{\pi} + \frac{\mu_F \kappa_A \sqrt{N}}{\sqrt{\pi}}(\sqrt{z}\, f_A(1-z))\right] \\
& +O(x^0)\ .
\end{aligned} \tag{31}
$$

In terms of $\tilde{f}(w)$, this is

$$
\begin{aligned}
0 = & \ \mu_F^2 - \frac{G^2}{2\pi}\left(1-\pi\alpha\cot(\pi\alpha)\right) \\
& -\frac{\kappa_S^2 N}{\pi}\int_0^1 \frac{\mathrm{d}w}{w}\left[\frac{(1+w)}{\sqrt{1-w}}\left(1-w+\tilde{f}_S(w)\right) - 1\right] \\
& -\frac{\kappa_A^2 N}{\pi}\int_0^1 \frac{\mathrm{d}w}{w}\left[\sqrt{1-w}\left(1-w+\tilde{f}_A(w)\right) - 1\right]\ .
\end{aligned} \tag{32}
$$

Using our numerical calculations of $f_S(w)$ and $f_A(w)$ we looked at α in terms of the other parameters; see Figures 2–5. Note that α is not defined for some areas of the parameter space, corresponding generally to large values of κ_S (Fig. 3). Also, note that α is very nearly constant with respect to μ_B, increasing only slightly with increased μ_B (Fig. 2).

Comments

1. The endpoint behavior is the same for both quarks and anti-quarks. Also, it is the same for each of the four states that we studied.

2. This analysis does not give the order of the states unambiguously, but it is clear that only the κ_A interaction splits the four states. I believe that the $J_z = 0$ component of the rho should have the highest energy because $\psi_A(x, y)$ has a node

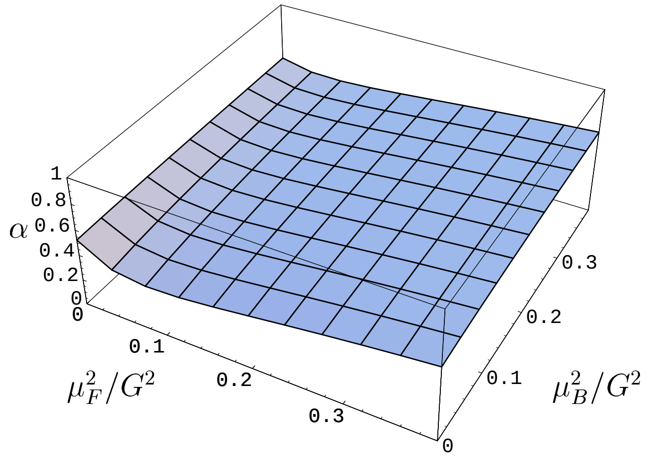

Figure 2: α vs. μ_F^2 and μ_B^2; $\kappa_S\sqrt{N} = -0.323G$, $\kappa_A\sqrt{N} = 0.162G$, $K = 25$.

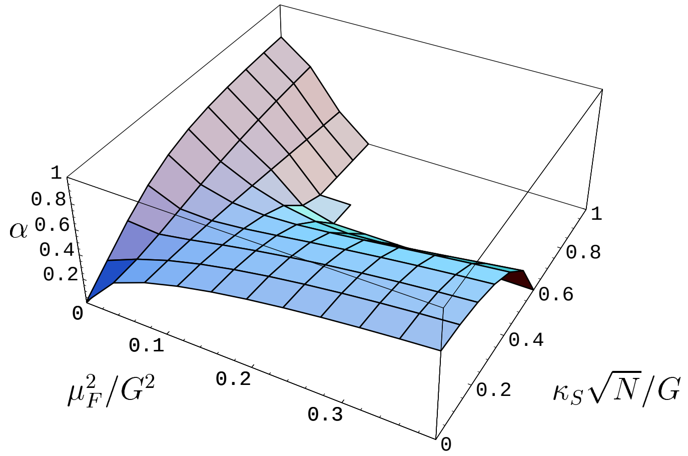

Figure 3: α vs. μ_F and κ_S; $\mu_B = 0.2G$, $\kappa_A = 0$, and $K = 25$.

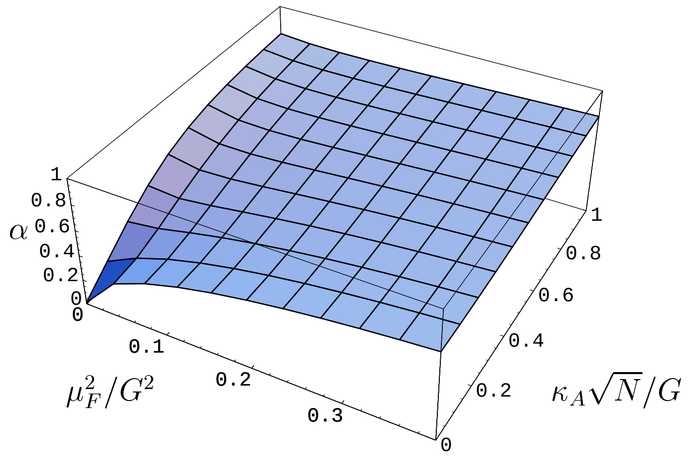

Figure 4: α vs. μ_F and κ_A; $\mu_B = 0.2G$, $\kappa_S = 0$, and $K = 25$.

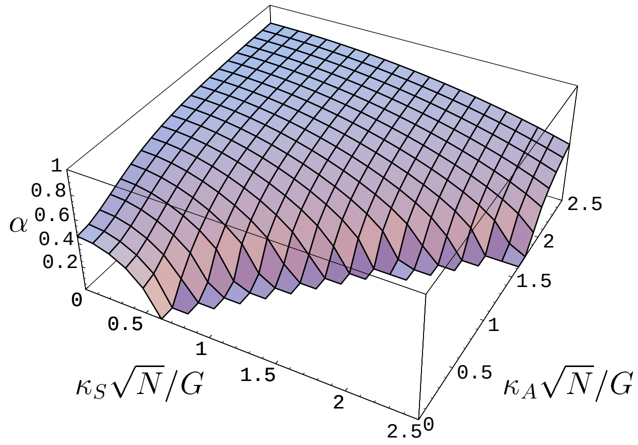

Figure 5: α vs. κ_S and κ_A; $\mu_F = 0.362G$, $\mu_B = 0.2G$, and $K = 25$.

at $x = 1 - x - y$. I think that the $J_z = \pm 1$ components of the rho should have the lowest energy, because they have more "phase space" to occupy. And the pion should have some energy in between the other two.

3. One could turn the equation for α into a recursion relation. One could use (30) & (32) to find α for a state with n particles and use a modification of (30) & (32) to find α for $n-1$ particle states.

4. We do need to extend this analysis to include two-link states: in that case, we could study the endpoint equation in the most general case.

5. We tried very hard to find a good variational ansatz for the wavefunction. The best we could come up with is

$$\psi(x) = C_2\, x^{\alpha}(1-x)^{\alpha} \tag{33}$$

$$\psi_{S,A}(x,y) = C_{S,A}\, \frac{y^{\beta}(1-y)^{\alpha}}{[(1-x)(x+y)]^{\beta+1/2-\alpha}} \tag{34}$$

However, even for this wavefunction, the necessary integrations are too difficult to perform. It is interesting to note that considerable simplification occurs when $\beta = \alpha - 1/2$.

6. According to the quantization procedure, the Fermion zero-modes — unlike the link zero-modes — are dynamical. However, according to Eqns. (22) and (23), these zero modes are constrained by the Yukawa interaction. I am puzzled by this inconsistency.

7. The $\lim_{x\to 0}\psi(x,y)$, y fixed, reminds me of one of the big themes in M-theory: The two-particle wavefunction lives on the boundary of the three-particle wavefunction.

8. Even for a DLCQ calculation, it seems that one might want periodic boundary conditions for the Fermions, and use (22) & (23) for the zero mode.

9. I think I see some tricks for handling the zero-modes for the link fields (without resorting to the constraint equation). For DLCQ, one can imagine 'almost' periodic boundary conditions:
$$M(x^-) = e^{i\epsilon} M(x^- + L) \tag{35}$$
This is equivalent to adding a background field in the x^- direction. (Coleman did something like this for the Schwinger model, I believe.) The idea here is that the zero-mode is represented by a very small momentum dynamical mode. When creating a basis of states, we would exclude any state with two zero-modes that are adjacent in the color string. For making "improved" matrix elements, we would define the zero-mode to be equal to the zero-momentum limit of the wavefunction: $\lim_{x_i \to 0} \psi(\ldots, x_i, \ldots)/x_i^\beta$. This is just an idea — I haven't worked out the details.

10. I am still in the middle of the calculation of the rho to 2-pion decay rate. We are going to have to find a way to make these calculations easier. I believe that we should write a Mathematica routine that finds matrix elements of the Hamiltonian at finite N. This will be a lot of work, but it could then be used on a large class of problems: decay widths, finite N corrections to eigenstates, *et cetera.*